STUDIES ON COLLAGEN

II. Cylindrical Lattice Structure of Collagen

By V. Sasisekharan and G. N. Ramachandran, F.A.Sc.

(*Department of Physics, University of Madras, Madras-25*)

Received March 25, 1957

1. Introduction

The main features of the structure of collagen at the molecular level have been reasonably well worked out (Ramachandran and Kartha, 1955; 1956). The polypeptide chains form three non-coaxial helices in the protofibril and are further wound up into coiled coils about a common axis. The three chains are attached to one another by means of hydrogen bonds approximately perpendicular to the fibre axis. These triple chain rods are arranged in a hexagonal array, the distance between them varying with the amount of moisture present. Though this structure explains fairly well the wide angle X-ray pattern of collagen, some of the details are not yet clear. The most puzzling aspect is the non-occurrence of the $11\bar{2}0$ (110) reflection or its analogue having the same ξ-value in the higher layers. It is usually supposed that the Fourier transform of the structure is weak in this region, and that the absence of a spot in the zero layer corresponding to the 110 reflection is due to this cause; but it is difficult to believe that it should be so for every layer line. In fact, a spot having roughly this ξ-value ($\xi = 0{\cdot}20$) occurs on the fourth layer line of kangaroo tail tendon and was identified as such by Ramachandran and Ambady (1954). However, the actually observed ξ-value differs from the expected value of 0·24 by an appreciable amount. Thus it would appear that the whole series of reflections of the type $11l$ is forbidden for collagen. Further it is found that the observed ξ-values in general lie close to 0·14, 0·28 and 0·42 in all the layer lines, *i.e.*, in the ratio of 1 : 2 : 3 and not at intermediate values like $\sqrt{3}$ or $\sqrt{7}$ times the basic unit of 0·14. This suggests that reflections with mixed indices of the type hk (both h and k non-zero) do not occur in the X-ray pattern of collagen.

Although a few spacings larger than 15 Å have been previously reported (Corey and Wyckoff, 1936) they had not been confirmed. Photographs taken in this laboratory of native cattle achilles tendon showed diffuse maxima at about 18 Å, 29 Å and 46 Å. These agreed with the observations of Corey and Wyckoff. The publication of a beautiful photograph taken by Cowan, North and Randall (1955), recording a whole series of sharp reflections in

this range brought to light the fact that the earlier observations were done at insufficient resolution. Even in this photograph the 110 reflection is missing on the equator. The fact that such a large number of sharp reflections are observed at small angles shows that the specimen is well oriented and it is therefore all the more surprising that no reflections were recorded corresponding to the ξ-value of the 110 spacing of the hexagonal lattice.

This difficulty is resolved and at the same time the occurrence of a large number of equatorial long spacings is also explained, if it is assumed that the structure of collagen is not built on a regular lattice, but on a cylindrical lattice. The idea of cylindrical and spiral lattices is briefly discussed below and they are applied to the case of collagen. It is very probable that these concepts could be extended to other fibrous proteins as well; some suggestive evidence in these cases is also presented.

2. General Theory of Cylindrical Lattice

A number of excellent theoretical papers have appeared on cylindrical lattices, their classification and their Fourier transform (Whittaker, 1954; 1955; Jagodzinski and Kunze, 1954; Waser, 1954). We shall consider here briefly the general theory of a simple normal cylindrical lattice. Such a cylindrical lattice is built up of a series of sheets, forming the surfaces of coaxial cylinders, the radii of these increasing in arithmetical progression. In any small region, it could be imagined as having been derived from a regular lattice by giving it a cylindrical curvature. Thus if ρ_m is the radius of the m-th cylinder and p_m the number of lattice points along its circumference, then $\rho_m = a_0 + ma$, a_0 being the radius of the innermost cylinder and $2\pi\rho_m = p_m b$, where b is the distance between the neighbouring points along the circumference. Suppose that the z-axis is along the axis of the coaxial cylinders; then any point can be defined by the cylindrical co-ordinates ρ, ϕ and z. Let the points which are nearest to the initial plane ($\phi = 0$) lying on the m-th cylinder have the co-ordinates $\phi = \delta_m$. Then the angular parameters ϕ of the points in the m-th cylinder are given by

$$\phi = \frac{bv}{p_m} + \delta_m$$

where v is an integer such that $1 \leqslant v \leqslant p_m$. Also $\rho = \rho_m = a_0 + ma$ and $z = nc$, where c is the repeat distance along the axis of the cylinder.

In accordance with the usual theory of diffraction, the amplitude of the diffracted wave along a direction given by the reciprocal vector $\mathbf{s}$ is the Fourier transform of these cylinders, which is given by

$$T = \sum_m \sum_n \sum_\nu \exp\left(\frac{2\pi i}{\lambda} \mathbf{r}.\mathbf{s}\right) \tag{1}$$

where $\mathbf{r}$ is the position vector. The vector $\mathbf{s}$ may be called the diffraction vector, whose terminus is given by the co-ordinates ρ^*, ϕ^* and z^*. Then,

$$\mathbf{r}.\mathbf{s} = \rho\rho^* \cos(\phi^* - \phi) - zz^* \tag{2}$$

Thus,

$$T = \sum_n \exp\left(\frac{2\pi i}{\lambda} ncz^*\right) \sum_m \sum_\nu \exp \frac{2\pi i}{\lambda} [\rho_m \rho^* \cos(\phi^* - \phi_{m\nu})] \tag{3}$$

Replacing the exponential functions occurring in the sum in expression (3) by a series of Bessel functions,

$$T = \sum_n \exp\left(\frac{2\pi i}{\lambda} ncz^*\right) \sum_m \sum_{q=-\infty}^{\infty} i^q J_q\left(\frac{2\pi}{\lambda} \rho_m \rho^*\right)$$

$$\times \exp[iq(\phi^* - \delta_m)] \sum_\nu \exp\left(-\frac{2\pi i q \nu}{p_m}\right) \tag{4}$$

The last sum, $\sum_\nu$, is finite only when $q = kp_m$ (where k is an integer) and it is then equal to p_m. It vanishes otherwise, so that,

$$T = \sum_n \exp\left(\frac{2\pi i}{\lambda} ncz^*\right) \sum_m p_m \sum_{q=-\infty}^{\infty} J_{kp_m}\left(\frac{2\pi}{\lambda} \rho_m \rho^*\right)$$

$$\times \exp\left[ikp_m\left(\phi^* + \frac{\pi}{2} - \delta_m\right)\right] \tag{5}$$

The first summation, $\sum_n$, has appreciable values only in the vicinity of planes in the reciprocal space, given by $z^* = l\lambda/c$, where l is an integer. These are the usual layer lines. In the second summation, $\sum_m$, the square of the modulus of the functions, averaged over rapid oscillations in ϕ^*, causes all cross terms between high order Bessel functions associated with different values of k, and cross terms between them and J_0, to vanish. Also, cross terms involving different m's tend to vanish unless $k = 0$. Thus when $k \neq 0$ the intensity $|T|^2$ is proportional to

$$\sum_{k=1}^{\infty} \sum_m p_m^2 J_{kp_m}^2\left(\frac{2\pi}{\lambda} \rho_m \rho^*\right) \tag{6}$$

This function has peaks corresponding to $\rho^* = k\lambda/b$ $(k = 1, 2, 3, \ldots)$, thus leading to characteristic bands of large intensity in reciprocal space on

cylinders, whose radii are multiples of b^*. The intensity of the k-th band arises essentially from the Bessel functions of orders $\pm kp_m$. From the expression (6), it is seen that the intensities due to the scattering from the component cylinders of the lattice are additive for these bands. These bands are known as the 'diffuse' series, since they are accompanied by a tail of secondary maxima on the longer ρ^* side.

When $k = 0$, however, there is interference between the terms $J_0(2\pi/\lambda \times \rho_m\rho^*)$ for different ρ_m and the amplitudes due to the component cylinders are additive. The intensity $|T|^2$ is proportional to

$$\left| \sum_m p_m J_0\left(\frac{2\pi}{\lambda} \rho_m\rho^*\right) \right|^2 \tag{7}$$

The intensity exhibits sharp maxima on bands corresponding to $\rho^* = h\lambda/a$ (h integral).

Thus, the diffraction pattern can be described as consisting of a series of layer lines at $\xi = l\lambda/c$, on which two series of reflections occur, one the sharp series at $\xi = h\lambda/a$ (h integral) and the other the diffuse series at $\xi = k\lambda/b$.

The above discussion is confined to the case in which the two-dimensional lattice inscribed on the cylindrical layers is primitive and rectangular and has one axis oriented perpendicular to the cylinder axis. Whittaker (1955) has enumerated and classified the possible types of cylindrical lattices and has extended the theory to diffraction by regular cylindrical lattices, with an oblique generating lattice and by those belonging to the helical series. A particular case of diffraction by a helical structure has also been discussed by Jagodzinski and Kunze (1954). These papers may be consulted for a more detailed account of the theory.

3. CYLINDRICAL LATTICE FOR COLLAGEN

Let us consider a cylindrical lattice built up of protofibrils* all running parallel to the axis of the cylinders. Then in any cross-section the appearance will be similar to Fig. 1, in which each protofibril is represented by a small circle. The distance between successive cylinders is a and if b is the distance between the protofibrils on any cylinder, then we have the result $\Delta n = n_j - n_{j-1} = 2\pi a/b$, where n_j is the number of protofibrils on the j-th cylindrical surface. This must obviously be an integer and the number was chosen to be six for collagen. The choice came from a consideration of the symmetry of coupling the cylinders together, and the occurrence of a regular

* The term protofibril is used for the elementary unit of the structure. This may consist of a single polypeptide chain as in the α-helix or a triple chain, as in the collagen structure.

hexagonal lattice as an approximation. This immediately imposed a relation between a and b, namely, that $2\pi a = 6b$ and thereby the geometry of the structure was completely fixed.

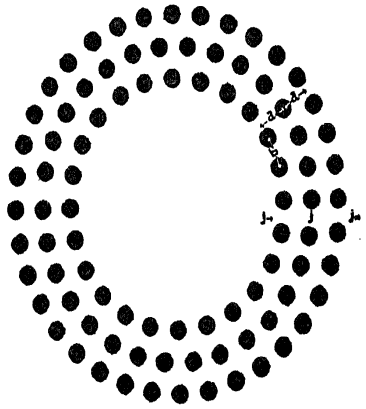

FIG. 1. Cross-section of a cylindrical lattice.

However, as one goes towards the centre, there are two possibilities in the central region, as indicated by Figs. 2 (*a*) and 2 (*b*). They are best described

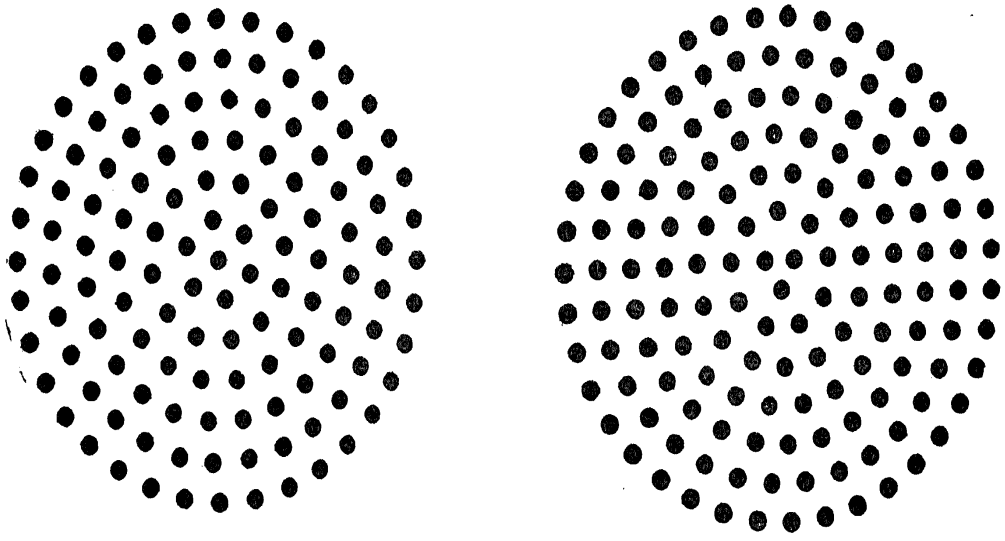

FIG. 2. The two possible cylindrical lattice structures of collagen. Each circle represents a protofibril. (*a*) Structure with one protofibril right at the centre. (*b*) Structure with three protofibrils forming an equilateral triangle at the centre.

by the relations (i) $a_j = ja$ and (ii) $a_j = (j - \frac{1}{2})\, a$. Thus Fig. 2 (*a*) has a protofibril right at the centre, while the innermost core in Fig. 2 (*b*) consists of three protofibrils forming an equilateral triangle. In both cases, the structure at the centre corresponds approximately to a regular hexagonal lattice and outside, it fits in with the scheme for a cylindrical lattice. The choice between the two could not be made on *a priori* grounds, but was possible from a detailed comparison with the equatorial long spacings in the X-ray pattern, which indicated that the structure shown in Fig. 2 (*b*) is the correct one. There is a reasonable fit with the data if the central protofibril is not there in the structure shown in Fig. 2 (*a*).

The c-axis of the structure was taken to be parallel to the cylinder axis, the repeat spacing being 28·6 Å, the value for the protofibril. From the properties of the transform of the cylindrical lattice, there will be maxima corresponding to $\xi = h\,\lambda/a = ha^*$ and $\xi = k\,\lambda/b = kb^*$ on the equator and on all layers defined by $\xi = l\,\lambda/c = lc^*$. In the present case, since $a/b = 2\pi/6 = 1{\cdot}047$, the two series of principal maxima (namely ha^* and kb^* series) practically coincide and only one set of principal reflections occur at $\xi = h\,\xi_0$ ($\xi_0 \simeq \lambda/a$). On the other hand, no reflections can occur at values of $\xi = ha^* + kb^*$, corresponding to mixed indices of the type h, k, with both h and k non-zero. Physically, this can also be explained as being due to the fact that, while there is a regular order among the points in any particular ring in Fig. 1 and also while the distance between any two circles is a constant, there is no correlation between the points in different circles in that figure. The points get in step and out of step periodically and so the analogue of a $hk0$ plane cannot occur.

Thus, while reflections of the type $h0l$ and $0kl$ are possible, those of the type $hk0$ and hkl cannot occur. In particular, 110 *is a forbidden reflection for collagen*, and this ξ-value cannot also occur in any of the layer lines. In fact, the absence of mixed h and k indices in the diffraction pattern of cylindrical lattices has been noticed in the case of chrysotile by Jagodzinski and Kunze (1954).

4. COMPARISON WITH THE OBSERVED EQUATORIAL LONG SPACINGS

The absence of the 110 reflection and its analogue in the other layers thus receives a natural explanation. However, the real evidence for the cylindrical lattice is obtained from a comparison of the calculated Fourier transform of the cylindrical lattice with the observed X-ray diffraction pattern. A number of subsidiary maxima occur at intermediate values of ξ in between the principal maxima. These have been worked out for the structure with seven cylindrical sheets [Fig. 2 (*b*)] and the results are shown in Table I for the region from 0 to ξ_0. The value of spacings larger than 10 Å observed on the equator and their relative intensities are given in columns 3 and 4 of Table I. The first and second columns contain the calculated spacings and intensities. The spacings were calculated taking the most intense reflection at 12·6 Å to correspond to the principal maximum of the first order. The number seven was arrived at by comparing the theoretical values with observations. The agreement between the calculated and observed values is seen to be good.

The sharpness of the observed maxima indicates that all the fibres in the specimen have exactly the same number of sheets. On drying the fibres,

TABLE I

Calculated and observed maxima in the diffraction pattern of a cylindrical lattice with 7 sheets

Calculated		Observed	
Spacing	Intensity (arbitrary units)	Spacing	Intensity
110	43·6	..	..
66	12·3	..	..
49·5	3·6	49·0	s
38	3·2	37·0	s
31·5	1·7	31·0	w
26·5	2·0	24·5	m
23·5	1·0		
20·5	1·8	20·5	w
18·5	1·0	18·8	m
16·8	3·2	17·0	m
15·4	2·9	14·9	m
13·9	38·0	13·5	v.s.
12·6*	93·0	12·6*	v.s.

* Adjusted to be equal.

this regularity is lost and on rewetting, only a streak joining the centre to the principal equatorial spots is observed. A similar streak is also observed in other layer lines, notably in the third layer line, showing that there is appreciable scattering power in the region in between the principal maxima. If the Fourier transform of the protofibril does not have a large value at the ξ-values corresponding to the principal maxima, but only in between, then it will record as a diffuse reflection on the particular layer line. The broad peak at $\xi = 0{\cdot}20$ in the fourth layer line is probably of this type.

In order to see the behaviour of the transform beyond the first principal maximum, the calculations were continued for the range from that to the second principal maximum for the structure with seven cylindrical sheets [Fig. 2 (*b*)]. From the cylindrical lattice theory, the intensity distribution along the equator, or zero layer, is given by

$$I(\xi) = c \left| \sum_{m=1}^{7} 3(2m-1)\, J_0\left(\pi (2m-1)\, \xi/a^*\right) \right|^2$$

$$+ 2c \left[\sum_{k=1}^{\infty} \sum_{m=1}^{7} 9(2m-1)^2 J^2_{3k(2m-1)}\left(3(2m-1)\, \xi/b^*\right) \right]$$

where c is a constant. A graph is shown in Fig. 3 connecting intensity and the ξ-value. The intensity calculations were made at intervals of $\pi\ \xi/a^*$

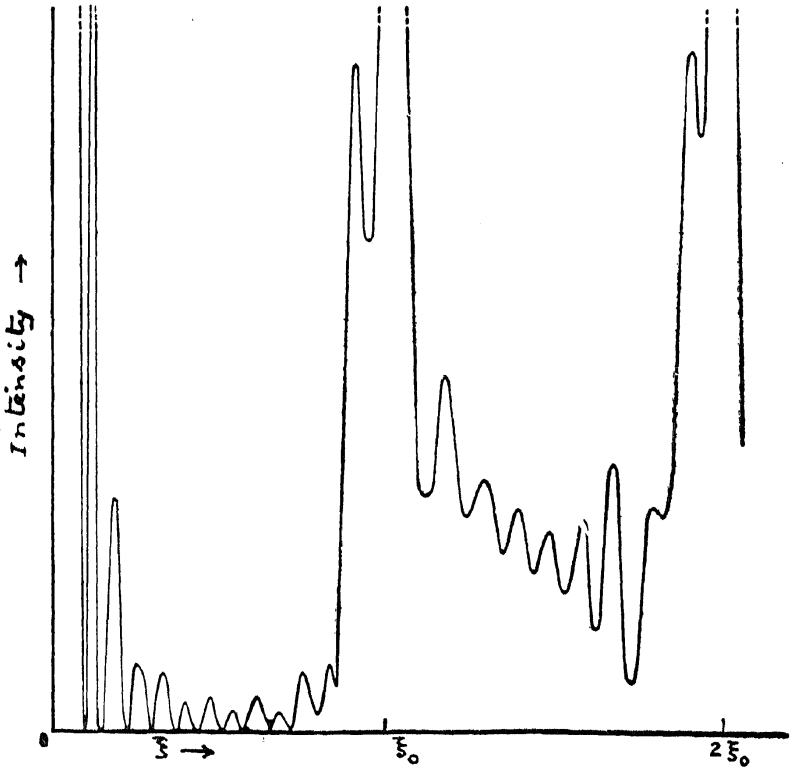

FIG. 3. A graph connecting the variation of intensity with ξ for the structure shown in Fig. 2 (*b*).

$= 3\xi/b^* = 0{\cdot}05$. The intensity variations in the range from 0 to ξ_0 ($\xi_0 \simeq \lambda/a$) is mainly due to the contribution by the first part of the above equation. The nature of the second function is such that it has appreciable values only when ξ approaches $k\,\xi_0$ and thereafter it is oscillatory in nature. The intensity however never falls to zero beyond ξ_0, so that sharp subsidiary maxima would not be observed. It must be noted that in general there is an appreciable scattering power in the region between any two principal maxima. This is a feature peculiar to the cylindrical lattice and does not occur with a regular lattice, even if the lattice is finite. With a finite regular lattice, the intensity distribution between any two principal maxima is the same and exhibits a number of subsidiary maxima, which fall away in intensity on moving away from a principal maxima. With a cylindrical lattice, this feature occurs only between zero and the first principal maxima. The diffuse intensity in the region between the principal maxima increases with increasing ξ-value.

There is thus clear evidence that the aggregation of collagen protofibrils is based on a cylindrical lattice and that they form cylindrical cryptofibrils of diameter approximately 200 Å [2× (13–15) × 7].† In fact fibrils of this

† The term "cryptofibril" is used to indicate cylindrical structures of the type discussed, with a diameter of the order of 200 Å.

order of diameter showing characteristic 640 Å axial period have been observed in the electron microscope. In particular, they are very clearly seen in the beautiful photographs reported by Swerdlow and Stromberg (1955) of fibrils subjected to mercury at high pressure. These pictures indicate that an ordinary fibril having a diameter of the order of 500–2000 Å is built up of such cryptofibrils. Burton *et al.* (1955) have found that fine threads, about 150–250 Å in diameter, are produced in the early stages of the degradation of collagen by chemical treatment.

5. The Possibility of Roll Structure

So far, we have discussed the cylindrical lattice structure. However, it seems physically more probable that a cylindrically curved layer structure would have for its cross-section a spiral, rather than a set of concentric circles. In that case, the complete structure can be obtained by rolling up a single sheet, in which the protofibrils form a parallel array.

In any cross-section, the equation to the spiral can be written in the form $r = k\theta$. As before, the whole structure can be characterised by two distances (i) the distance a between the sheets and (ii) the distance b between the protofibrils in the sheet. We may assume, to start with, that the sheet is rolled about an axis parallel to the protofibrils. If this were not so, the protofibrils would take up the configuration of a helix, whose radius is continuously increasing. So far, it has not been possible to work out theoretically the diffraction pattern of a spiral lattice, even of the simple type. However, by an experimental approach described in the next section, it is found that the rotated Fourier transform is of the same type as the one obtained from a cylindrical lattice.

The spiral lattice appropriate to collagen is shown in Fig. 4. Here also, the relation $2\pi a = 6b$ was used for plotting the lattice points. The lattice

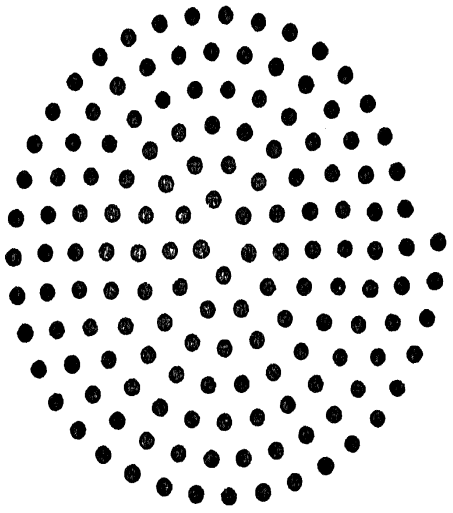

Fig. 4. Cross-section of a roll structure (spiral lattice) appropriate to collagen.

points were so plotted that the spiral structure thus obtained broadly resembled the one shown in Fig. 2 (*b*).

6. OPTICAL TRANSFORMS OF CYLINDRICAL LATTICE STRUCTURE OF COLLAGEN

The above results of the cylindrical and spiral lattice structures were confirmed by means of experiments, made on models with an optical diffractometer. The diffraction apparatus used in these experiments was the one described by Aravindakshan (1957). As with other optical diffraction apparatus, this also does not permit the study of diffraction patterns from three-dimensional objects. So investigations were carried out only of diffraction from plane circular and spiral lattices. However, for the present purpose, this does not involve any limitations, since the diffraction pattern obtained from such a lattice is equivalent to the distribution of intensity on the zero layer plane in reciprocal space for the corresponding cylindrical lattice.

The pinhole source used was 40 microns in diameter and the resolution was fairly high. Photographic etched masks (Aravindakshan, 1957) were used at the beginning of the experiment. Because of the non-uniformity of the photographic glass plate, distortions were produced in the image. A more serious difficulty was a displacement due to the non-parallelism of the two surfaces of the glass plate, as a result of which rotated optical transforms could not be recorded. The masks were later prepared using a pantograph punch on a scale 0·185 mm./Å. Each lattice point was represented by a hole 0·45 mm. in diameter. The first minimum of the diffraction pattern from a hole of this size occurs at $\xi = 0{\cdot}75$, which is well beyond the range ($\xi < 0{\cdot}30$) of the optical transform useful for study. These holes were punched on a blackened photographic film. The drawings, from which the masks were prepared, were constructed on a scale nine times larger. In order to plot the points of the lattice, their loci (either concentric circles or the spiral, as the case may be) were drawn first. The lattice points were then set off at equal distances along the curve, their positions being checked and corrected at least every 90°. The optical transforms were photographed directly on a fine grain photographic plate and enlarged for reproduction.

A comparison with the X-ray results can be best had when the transform is obtained with the mask continuously rotated in the optical diffraction apparatus. The transform thus obtained may be called 'rotated transform' and for a satisfactory result, neither accurate centering of the mask nor absolute uniformity of motion is required. The only requirement is that

the plane of the mask must remain the same during rotation and this is readily achieved by using a good ball-bearing.

(*a*) *Cylindrical lattice.*—The optical transforms obtained for the two possible cylindrical lattice structures of collagen [(Figs. 2 (*a*) and 2 (*b*)] are shown in Figs. 5 and 6, along with their rotated transforms. The similarity between the two transforms is remarkable. In both cases, the six-fold symmetry of the pattern arises from the relation $2\pi a = 6b$. The sharpness of the maxima, their fine structure and the arch-like distribution of the diffuse reflections are all to be expected from theory.

The two rotated transforms contain rings of large intensity only at integral multiples of a unit and not at multiples like $\sqrt{3}$, $\sqrt{7}$, etc., which would be expected for a simple hexagonal lattice. The distinction between the cylindrical lattice and a simple hexagonal lattice of the same dimensions is easily seen by comparing their rotated transforms shown in Figs. 6 (*b*) and 7 (*b*). The absence of rings corresponding to the reflections 1, 1 and 2, 1 with the cylindrical lattice is particularly noteworthy and supports the theoretical prediction.

A number of weak rings (subsidiary maxima) are found in the rotated transform of the lattices, and are particularly clear in the central region inside the first ring. However, their number and spacings differ, *e.g.*, they are quite different for the two types of cylindrical lattice structures discussed here. In fact, it was the number and spacings of the subsidiary maxima near the central region which enabled the authors to choose the structure shown in Fig. 2 (*b*) as the proper one. The spacing of the rings for this structure are shown in Table II in the second column. The agreement between this and the observed spacings is seen to be good. In the photographs reproduced, only the stronger among the subsidiary maxima are clearly seen.

(*b*) *Spiral lattice.*—The optical transforms of the spiral lattice appropriate to collagen are shown in Fig. 8. The similarity between these and the transforms of the cylindrical lattices is striking; however, the symmetry is only approximately six-fold in this case. In the ordinary transform many of the spots making up the pattern do not lie in exactly the same positions on the various arches, a fact which clearly arises from the spiral character of the lattice.

As before, the rotated transform contains intense rings only at integral multiples of a unit. The spacings of the subsidiary maxima near the central region obtained from this lattice are given in Table II in the third column. The agreement between this and the observed spacings is again good. A

TABLE II

Observed spacings (in A*) in the X-ray diffraction pattern of collagen and the spacings calculated from measurements on the diffraction pattern of cylindrical and spiral lattices in an optical diffractometer*

From X-ray pattern	From rotated transform of	
	Cylindrical lattice	Spiral lattice
..	101	99
..	67	65
49·0	49·0	49
37·0	38·0	39
31·0	32·0	32
24·5	27·0	27
	24·0	23
20·5	21·0	20
18·8	..	..
17·0	17·0	17·3
14·9	15·4	14·8
13·5	14·2	14·0
12·6	12·6	12·6

comparison of the rotated transforms of the cylindrical and spiral lattices shows that there is more of intensity in between the principal maxima with the spiral lattice. This is to be expected, since there is less order in a spiral lattice than in a cylindrical lattice. The phenomenon is seen particularly well in the region between the first and second principal maxima in Fig. 8 (*b*). Thus all the evidences available so far are in accord with spiral lattice also, with the added advantage that the formation of a roll in the form of a continuous sheet is much more reasonable.

It is quite possible now that collagen has definitely been shown to have a cylindrical lattice structure, that other fibrous proteins also may have such a structure. This is particularly to be expected since the number of spots found in their X-ray pattern are very small, *e.g.*, in keratin, compared to those found in the patterns of some polypeptides. In fact, the published X-ray pattern of sea-gull feather keratin (Bear and Rugo, 1951) clearly indicates the occurrence of a cylindrical lattice. Only row lines corresponding to $h\,\xi_0$ are found with $h = 1, 2, 3, 4$ and $\xi_0 = 0{\cdot}045$. The absence of any other intermediate row lines of sharp spots clearly shows that a cylindrical lattice structure is present and also that the ratio a/b is probably the same as in

collagen. There is also an extension of reflecting power in some layer lines in between the principal row lines. Probably the α-keratin group also has this structure, as only one type of repeat spacing has been found along the equator.

Summary

It is suggested that the structure of collagen is based on a cylindrical lattice. The protofibrils, consisting of triple chains, are packed together in a hexagonal array close to the centre, and are extended outwards in the form of cylindrical sheets. Each sheet has a pseudohexagonal symmetry about the common axis. This cylindrical lattice explains (*a*) the large number of equatorial reflections of long spacings observed in the diffraction pattern of native fibres and (*b*) the absence of the 110 reflection and its analogue in all layer lines. The number of sheets in a single cylindrical rod is about 7 and its diameter about 200 Å.

The above results were verified by model optical diffraction experiments. Also, from these experiments it is shown that the structure can also belong to the roll type with the added advantage that the formation of a roll in the form of a continuous sheet is more probable from the point of view of fibrogenesis.

References

1. Aravindakshan, C. .. *J. Sci. Instrun.*, 1957 (in press).
2. Bear, R. S. and Rugo, H. J. *Ann. N.Y. Acad. Sci.*, 1951, **53**, 627.
3. Burton, D., Hall, D. A., Keech, M. K., Reed, R., Saxl, H. and Tuhbridge, R. E. *Nature*, 1955, **176**, 966.
4. Corey, R. B. and Wyckoff, R. W. G. *J. Biol. Chem.*, 1936, **114**, 407.
5. Cowan, P. M., North, A. C. T. and Randall, J. T. *Symp. Soc. Exptl. Biol.*, 1955, **9**, 115.
6. Jagodzinski, H. and Kunze, G. *Neues Jb. Miner. Mh.*, 1954, 95, 113, 137.
7. Ramachandran, G. N. and Ambady, G. K. *Curr. Sci.*, 1954, **23**, 349.
8. ——— and Kartha, G. .. *Proc. Ind. Acad. Sci.*, 1955, **42 A**, 215.
9. Ramachandran, G. N. .. *Nature*, 1956, **177**, 710.
10. Swerdlow, M. and Stromberg, R. R. *J. Res. Nat. Bur. Stds.*, 1955, **54**, 83.
11. Waser, J. .. *Acta Cryst.*, 1954, **8**, 142.
12. Whittaker, E. J. W. .. *Ibid.*, 1954, **7**, 827; 1955, **8**, 261, 265, 571, 726.

EXPLANATION OF PLATE X

FIG. 5. Transforms of the structure shown in Fig. 2 *a*. (*a*) Ordinary transform, (*b*) Rotated transform.

FIG. 6. Transforms of the structure shown in Fig. 2 *b*. (*a*) Ordinary transform, (*b*) Rotated transform.

FIG. 7. Transforms of a simple hexagonal lattice. (*a*) Ordinary transform, (*b*) Rotated transform.

FIG. 8. Transforms of the spiral lattice shown in Fig. 4. (*a*) Ordinary transform, (*b*) Rotated transform.

FIG. 5 (*a*)

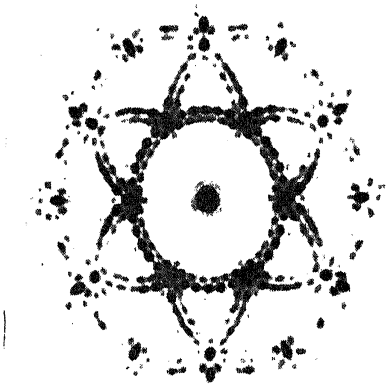

(*b*)

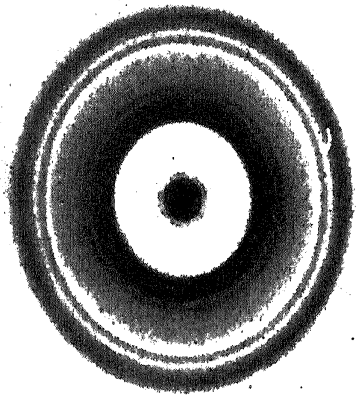

FIG. 6 (*a*)

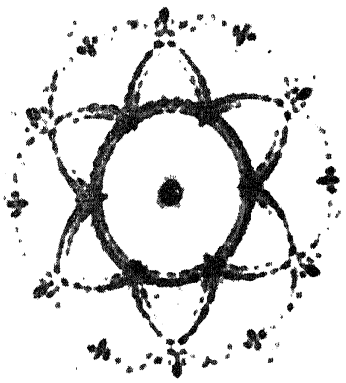

(*b*)

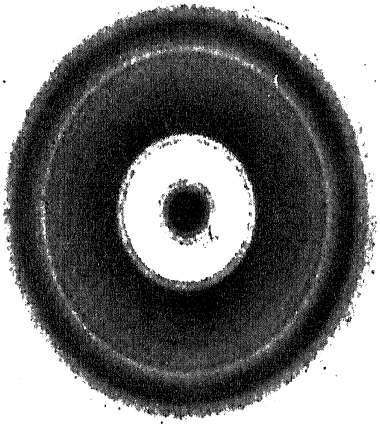

FIG. 7 (*a*)

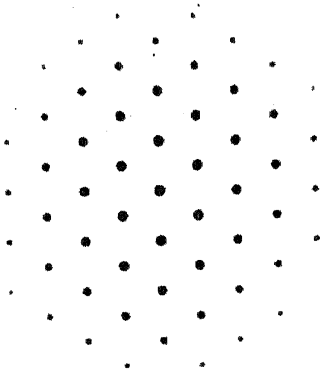

(*b*)

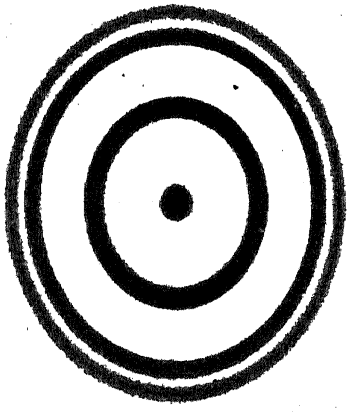

FIG. 8 (*a*)

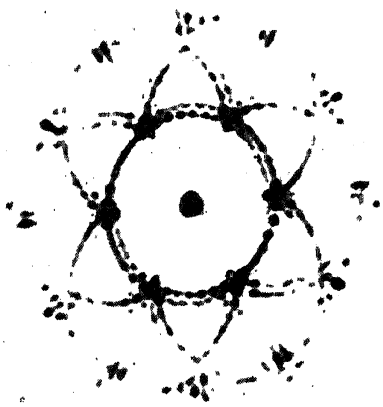

(*b*)